Development of a Novel Multiparametric MRI Radiomic Nomogram for Preoperative Evaluation of Early Recurrence in Resectable Pancreatic Cancer

Tian-Yu Tang, MD,[1,2,3#] Xiang Li, MD, PhD,[1,2,3#] Qi Zhang, MD, PhD,[1,2,3] Cheng-Xiang Guo, MD,[1,2,3] Xiao-Zhen Zhang, MD,[1,2,3] Meng-Yi Lao, MD,[1,2,3] Yi-Nan Shen, MD,[1,2,3] Wen-Bo Xiao, MD,[4] Shi-Hong Ying, MD,[4] Ke Sun, MD,[5] Ri-Sheng Yu, MD,[7] Shun-Liang Gao, MD,[1,2,3] Ri-Sheng Que, MD,[1,2,3] Wei Chen, MD, PhD,[1,2,3] Da-Bing Huang, MD,[1,2,3] Pei-Pei Pang, PhD,[6] Xue-Li Bai, MD, PhD,[1,2,3*] and Ting-Bo Liang, MD, PhD[1,2,3*]

Background: In pancreatic cancer, methods to predict early recurrence (ER) and identify patients at increased risk of relapse are urgently required.
Purpose: To develop a radiomic nomogram based on MR radiomics to stratify patients preoperatively and potentially improve clinical practice.
Study Type: Retrospective.
Population: We enrolled 303 patients from two medical centers. Patients with a disease-free survival ≤12 months were assigned as the ER group (n = 130). Patients from the first medical center were divided into a training cohort (n = 123) and an internal validation cohort (n = 54). Patients from the second medical center were used as the external independent validation cohort (n = 126).
Field Strength/Sequence: 3.0T axial T_1-weighted (T_1-w), T_2-weighted (T_2-w), contrast-enhanced T_1-weighted (CET_1-w).
Assessment: ER was confirmed via imaging studies as MRI or CT. Risk factors, including clinical stage, CA19-9, and radiomic-related features of ER were assessed. In addition, to determine the intra- and interobserver reproducibility of radiomic features extraction, the intra- and interclass correlation coefficients (ICC) were calculated.
Statistical Tests: The area under the receiver-operator characteristic (ROC) curve (AUC) was used to evaluate the predictive accuracy of the radiomic signature in both the training and test groups. The results of decision curve analysis (DCA) indicated that the radiomic nomogram achieved the most net benefit.
Results: The AUC values of ER evaluation for the radiomics signature were 0.80 (training cohort), 0.81 (internal validation cohort), and 0.78 (external validation cohort). Multivariate logistic analysis identified the radiomic signature, CA19-9 level, and clinical stage as independent parameters of ER. A radiomic nomogram was then developed incorporating the CA19-9 level and clinical stage. The AUC values for ER risk evaluation using the radiomic nomogram were 0.87 (training cohort), 0.88 (internal validation cohort), and 0.85 (external validation cohort).

View this article online at wileyonlinelibrary.com. DOI: 10.1002/jmri.27024

Received Sep 25, 2019, Accepted for publication Nov 27, 2019.

*Address reprint requests to: T.-B.L. or X.-L.B., 79 Qingchun Road, Hangzhou 310009, China. E-mail: liangtingbo@zju.edu.cn or shirleybai@zju.edu.cn
#These authors contributed equally to this work.

From the [1]Department of Hepatobiliary and Pancreatic Surgery, First Affiliated Hospital, Zhejiang University School of Medicine, Hangzhou, China; [2]Zhejiang Provincial Key Laboratory of Pancreatic Disease, Hangzhou, China; [3]Innovation Center for the Study of Pancreatic Diseases, Zhejiang Province, China; [4]Department of Radiology, First Affiliated Hospital, Zhejiang University School of Medicine, Hangzhou, China; [5]Department of Pathology, First Affiliated Hospital, Zhejiang University School of Medicine, Hangzhou, China; [6]GE Healthcare China, Shanghai, China; and [7]Department of Radiology, Second Affiliated Hospital, Zhejiang University School of Medicine, Hangzhou, China

Additional supporting information may be found in the online version of this article

Data Conclusion: The radiomic nomogram can effectively evaluate ER risks in patients with resectable pancreatic cancer preoperatively, which could potentially improve treatment strategies and facilitate personalized therapy in pancreatic cancer.
Level of Evidence: 4
Technical Efficacy: Stage 4

J. MAGN. RESON. IMAGING 2020;52:231–245.

PANCREATIC CANCER (PC) is one of the most lethal malignancies.[1] For patients with resectable disease, initial surgery combined with adjuvant chemotherapy are the first-line treatments. However, the prognosis of these patients is still poor and early recurrence (ER) is observed in 35–50% patients within 1 year after surgery.[1–3] Hence, evaluation of ER risk and identifying those patients with increased risk of relapse are necessary and urgent.

Imaging studies provide valuable information to predict ER after surgery in a wide range of malignancies. Conventional criteria, such as the tumor-node-metastasis (TNM) staging system, stratify patients using three major parameters on images: primary tumor, regional lymph nodes, and distant metastases.[4] Although these imaging criteria are fundamental to establish a prognostic risk evaluation, their application is limited. Moreover, there was a significant difference in survival among patients in identical stages.[4,5] One explanation is that conventional criteria mainly focus on the anatomical radiological features. This might oversimplify the complexity of a tumor's biological behavior, which is highly correlated with ER in patients. Therefore, the current stratification system needs to be improved and the identification of patients with increased risk of recurrence remains challenging for surgeons and oncologists.

In 2012, Lambin et al first presented the concept of "Radiomics."[6] The conventional criteria mainly focus on the anatomical radiological features. This might oversimplify the complexity of tumor improvement and behavior. Radiomics focuses on improvements of image analysis, using an automated high-throughput extraction of large amounts of quantitative features of medical images. It provides more and better information than that of a conventional approach.[6] Hundreds of quantitative features could be extracted from original imaging using a high-throughput approach and could be further analyzed. Recently, research has revealed the links between radiomics and underlying tumor biology in a wide range of malignant diseases, which are strongly correlated with tumor phenotype, aggressiveness, response to treatment, and prognosis.[7–10] Previous studies have shown that radiomics has the potential to predict ER in such malignancies as chondrosarcoma, hepatocellular carcinoma, and cholangiocarcinoma, which indicated that radiomics might provide surgeons with useful information in the anticipated era of precision medicine.[11–13] Kaissis et al recently developed several machine-learning models for the prediction of survival in PC based on radiomics features. The results showed that radiomics features were significantly associated with molecular subtypes of PC.[14,15] While these results are promising and encouraging, radiomic research in recurrence risk of PC is limited, which may due to limited data in current studies.

In this study we aimed to develop a radiomic feature-based nomogram to stratify resectable PC patients with high ER risks preoperatively. This model could provide surgeons with valuable information and potentially serve as reliable reference for clinical practice.

Materials and Methods

Patients

Data were obtained from medical centers A and B. This study was approved by Institutional Review Board of two centers. Between April 2012 to July 2018, patients who were diagnosed with PC and further underwent upfront surgery in the two institutions were included in this study. The exclusion criteria were: 1) Patients who did not receive a magnetic resonance imaging (MRI) scan within two weeks before surgery. 2) Patients lacking complete clinical data. 3) Patients lacking complete follow-up data. 4) Patients who were restaged as borderline resectable pancreatic cancer (BRPC) and locally advanced pancreatic cancer (LAPC) postoperatively. 5) Patients who died from surgical complications within 30 days after surgery. The inclusion criteria were met by 303 patients who were then enrolled in this study. A flowchart of this study is shown in Fig. 1. Patients were then divided into an ER group (disease-free survival ≤12 months) and a nonearly recurrence (NER) group (disease-free survival >12 months) according to previous studies, which indicated an optimal cutoff of 12 months for identifying the ER group and late recurrence group based on overall survival and survival after recurrence.[1,2] The preoperation MRI scans of the included patients were used to extract the radiomic features. The training cohort and internal validation cohort comprised patients from medical center A treated between April 2012 to July 2018. Patients from medical center B treated between April 2012 to July 2018 were included as the external validation cohort.

Clinical Data and Follow-up

The included patients were evaluated by a multidisciplinary team that comprised oncologists, radiologists, and surgeons. The clinical parameters including gender, age, symptoms, clinical stage, location of the tumor, laboratory examination results, surgical margin, and tumor differentiation were extracted from the electronic medical records system. The tumors' clinical stage was assessed using the AJCC guidelines (8th ed.).[4] Chest high-resolution computed tomography (HRCT), contrast-enhanced MRI, and abdominal contrast-enhanced computed tomography (CE-CT) were performed every 2 months during the first year after surgery. Serum tumor biomarkers were tested every month after surgery. Once CT or MRI showed a sign of new local or distant lesion, the recurrence was

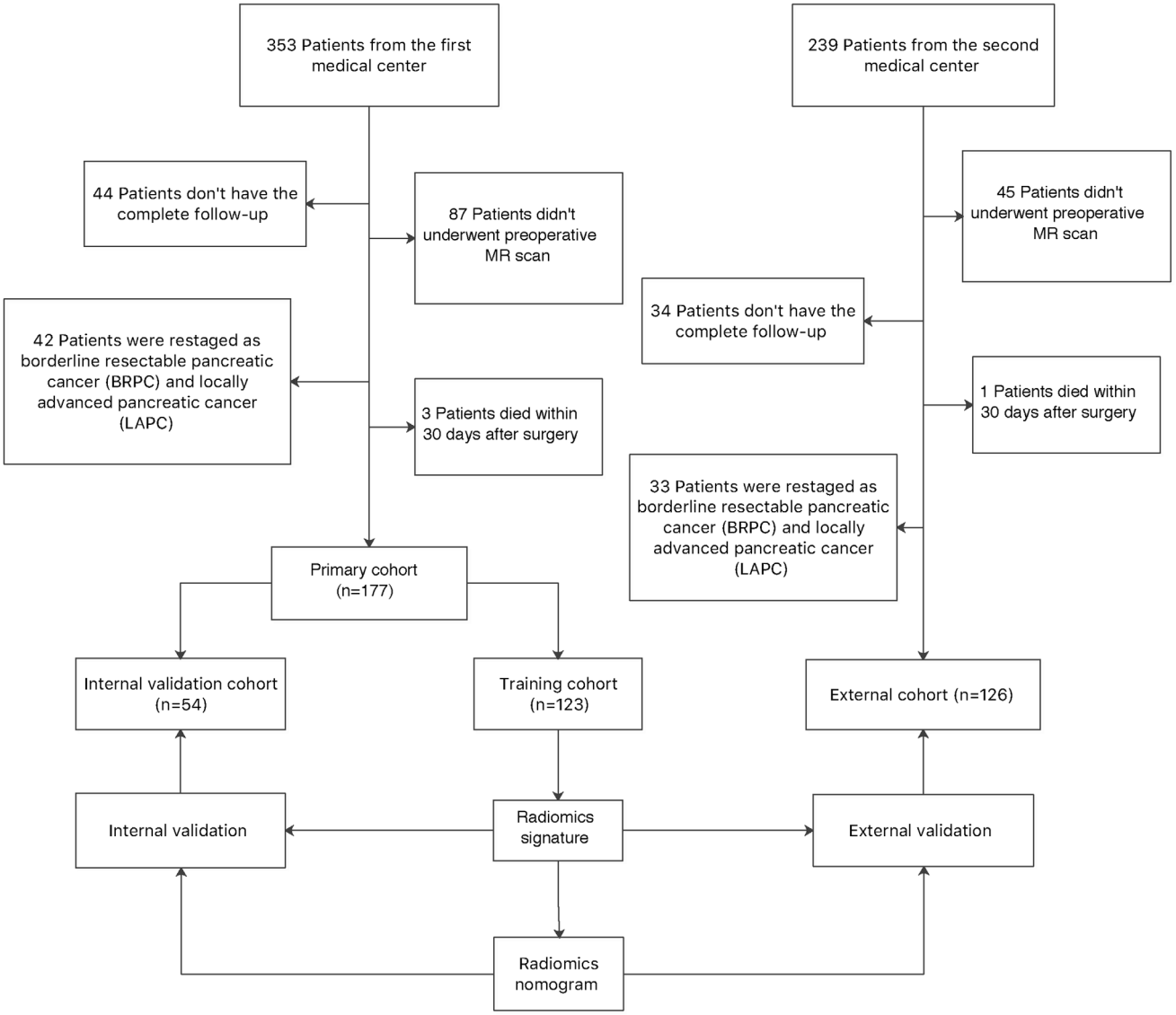

FIGURE 1: Flowchart showing the patient inclusion criteria and the study design.

confirmed. The status and the time was recorded as the date of first CT or MRI that showed disease progression.

MR Image Acquisition

All imaging data include four sets of images from three different scans: Preoperative T_1-w, T_2-w, CET_1-w arterial phase, and CET_1-w portal venous phase MR images. The T_1-w and CET_1-w images were acquired under breath-hold and T_2 image were acquired with a respiratory trigger.

In center A, preoperative MRI was performed with a 3.0T MR scanner (Discovery MR 750; GE Healthcare, Waukesha, WI). The parameters were as follows: T_1-w: repetition time (TR) = 4.1 msec, echo time (TE) = 2.4 msec, slice thickness = 3 mm, matrix = 260 × 224, and field of view (FOV) = 36*36 cm; T_2-w: TR = 12,000 msec, TE = 72 msec, slice thickness = 3 mm, matrix = 320*320, and FOV = 36*36 cm; Contrast-enhanced imaging was performed following the intravenous injection of 0.1 mmol/kg contrast medium (Gadodiamide, GE Healthcare), rate = 2 mL/s. The arterial phase and portal venous phase (20 and 60 sec postinjection, respectively) were collected. TR = 3.9 msec, TE = 2.2 msec, slice thickness =3 mm, matrix = 260*224, and FOV = 36 × 36 cm.

In center B, preoperative MRI was performed with a 3.0T system (Discovery MR750; GE Healthcare). The parameters were as follows: T_1-w: TR = 3.9 msec, TE = 1.2 msec, the slice thickness = 3 mm; matrix = 256 × 256, and FOV = 38*38 cm. T_2-w: TR = 6000–8000 msec, TE = 91 msec, slice thickness = 4 mm; matrix = 256 × 256, and FOV = 38*38 cm. Contrast-enhanced imaging was performed following the intravenous injection of 0.1 mmol/kg contrast medium (Gadodiamide, GE Healthcare), rate = 2 mL/s. The imaging delay time for arterial phase and portal venous phase was 20 sec and 50 sec, respectively. TR = 3.8 msec, TE = 1.7 msec, FOV = 380 × 300 mm, matrix = 320*224, slice thickness = 3.2 mm.

Region of Interest and Segmentation and Extraction of Radiomic Features

Preoperative T_1-w, T_2-w, arterial phase imaging, and portal venous phase imaging were used to extract the features (Supplemental Fig. 5). The AK software (Artificial Intelligence Kit v. 3.1.0.A, GE

Healthcare) was used to process the images before extracting the features. The Supplemental Material shows the details of imaging preprocessing. The regions of interest (ROIs) were manually contoured on MR by the radiologists. Contrast-enhanced CT was used as the reference. The two radiologists (X.W.B. and Y.S.H.), who both had more than 10 years experience of interpreting abdominal images, were blinded to the clinical outcome before ROI segmentation. All ROIs were segmented using ITK-SNAP v. 3.6.0 from UPenn (www.itksnap.org).[16] In total, 328 radiomic features were extracted from each MRI sequence using the AK software. The radiomic features extracted included: histograms, form factor parameters, GLCM (gray level co-occurrence matrix), and RLM (run length matrix). All extracted radiomic features were individually subtracted by the mean value of each feature and divided by the respective standard deviation values (Z-score normalization), thus removing the limitations imposed by the units of each feature. In the primary cohort, patients were randomly divided into two groups comprising the training set (n = 123) and the internal validation set (n = 54), with a proportion of 7:3. From the training set, the most useful predictive radiomic features were selected using LASSO (least absolute shrinkage and selection operator) regression, which is suitable for the regression of high-dimension data. The details of the features selection are shown in the Supplemental Material. After the optimal radiomic features were selected from the training set, a linear combination of selected features weighted by their respective coefficients were used to calculate a radiomic signature to predict ER after surgery for each patient. The area under the receiver-operator characteristic (ROC) curve (AUC) was used to evaluate the predictive accuracy of the radiomic signature in both the training and testing groups.

Intraobserver and Interobserver Agreement

To determine the intra- and interobserver reproducibility of radiomic features extraction, the intra- and interclass correlation coefficients (ICC) were calculated. Thirty images were chosen randomly for ROI segmentation by two radiologists who both had more than 10 years experience of interpreting abdominal images. The performances of two radiologists (A and B) were used to assess the interobserver ICC. The performance of one radiologist (A), who repeated the segmentation of the tumors, was used to assess the intraobserver ICC. An ICC greater than 0·8 was considered to represent good agreement of the feature extraction.

Radiomic Nomogram Development

Univariate logistic regression was first used to identify potential predictors. Then multivariate logistic regression was used to select the independent predictors of ER, which were subsequently used to develop a novel radiomic nomogram. The training and validation cohorts were used to test the calibration and discrimination performances of the radiomic nomogram. A calibration curve displayed the agreement between the predicted and observed risks of ER and was used to assess the calibration performance. The AUC was used to measure the discrimination performance. The radiomic nomogram was validated using the independent validation cohort of 126 patients from the second hospital.

Decision curve analysis (DCA) was used to assess the clinical utility of the radiomic nomogram model in the three cohorts (training, internal, and independent validation). The "true" positive and weighted false-positive rates were calculated across different threshold probabilities in the validation set to determine the net benefit. Specifically, the weighting factor was defined as the specific value of the threshold probability divided by 1 minus the threshold probability. A higher true-positive rate and a relatively low false-positive rate were suggested by a high net benefit. Plotting the net benefit against the threshold probability across the range of 0 to 0·8 generated the decision curve. We also plotted the DCA for the radiomic signature.

Statistical Analysis

Continuous variables are expressed as mean and standard deviation (SD), whereas categorical variables are expressed as the

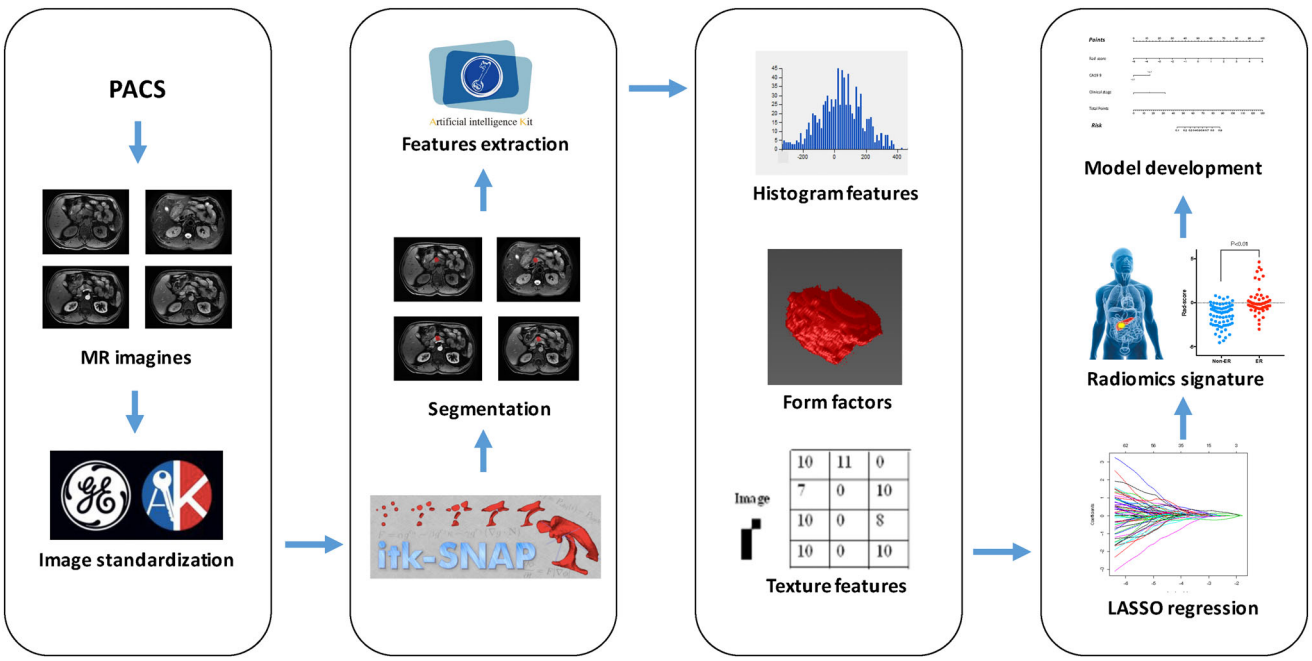

FIGURE 2: Workflow of the development of the radiomic signature.

TABLE 1. Characteristics of the Study Population

Parameters	Training cohort (*n* = 123)		Internal validation cohort (*n* = 54)		External validation cohort (*n* = 126)		*P* value
	n	%	*n*	%	*n*	%	
Age, years							0.839
≥ 60	71	57.7	33	61.1	71	56.3	
< 60	52	42.3	21	38.9	55	43.7	
Gender							0.859
Male	83	67.5	35	64.8	81	64.3	
Female	40	32.5	19	35.2	45	35.7	
Location							0.403
Proximal	90	73.2	38	70.4	93	73.8	
Distal	33	26.8	16	29.6	33	26.2	
Pain							0.414
Yes	76	61.8	33	61.1	68	54.0	
No	47	38.2	21	38.9	58	46.0	
Weight loss							0.847
Yes	61	49.6	29	53.7	62	49.2	
No	62	50.4	25	46.3	64	50.8	
CA199, kU/L							0.636
Normal	44	35.8	22	40.7	42	33.3	
Elevated	79	64.2	32	59.3	84	66.7	
CEA, ng/mL							
Normal	102	82.9	46	85.2	104	82.5	0.906
Elevated	21	17.1	8	14.8	22	17.5	
TB, μmol/L							
Normal	65	52.8	28	51.9	76	60.3	0.403
Elevated	58	47.2	26	48.1	50	39.7	
Albumin, g/L							
Normal	85	69.1	41	75.9	85	67.5	0.520
Decreased	38	30.9	13	24.1	41	32.5	
Stage							0.541
I	49	39.8	21	38.9	39	31.0	
II	61	49.6	26	48.1	67	53.2	
III	13	10.5	7	12.9	20	15.9	
IV	0	0	0	0	0	0	
Adjuvant chemotherapy							0.459
Yes	72	58.5	35	64.8	83	65.9	

TABLE 1. Continued

Parameters	Training cohort (n = 123)		Internal validation cohort (n = 54)		External validation cohort (n = 126)		P value
	n	%	n	%	n	%	
No	51	41.5	19	35.2	43	34.1	

TB: total bilirubin; CEA: carcinoembryonic antigen.
*$P < 0.05$.

frequency and proportion. The chi-squared test or Fisher's exact test were used to analyze the categorical variables, when appropriate. The Mann–Whitney *U*-test, or independent-sample *t*-test were used to assess the continuous variables, when appropriate. Penalty parameter tuning combined with the LASSO logistic regression model were performed using 10-fold cross-validation based on the minimum criteria. The likelihood ratio test was used for backward stepwise selection, which used Akaike's information criterion (AIC) as the stopping rule. Certain statistical analyses were conducted using R software (v. 3.5.1, Vienna, Austria). The "glmnet" package in R was used to perform LASSO logistic regression. The "rms" package was used for nomogram construction and calibration plotting. ROC plots were constructed using the "pROC" package. The "rmda" package was used to construct the DCA curve plots. The "rms" package in R was used to calibrate the radiomic signature using the calibration curve. SPSS 18.0 (IBM, Armonk, NY) and MedCalc software v. 15.2.2 (https://www.medcalc.org/) were used to perform the statistical analysis. Statistical significance was accepted at $P < 0.05$.

Results

Characteristics of the Patients

This study included 303 patients and flowcharts of the study are shown in Figs. 1 and 2. A total of 177 patients from the first medical center were divided into a training cohort (n = 123) and an internal validation cohort (n = 54). Patients from the second medical center were used as the external independent validation cohort (n = 126). Tables 1 and 2 show the patients' characteristics. Between the two centers, no difference in the ER rate was observed (74/177, 42.4% vs. 55/126, 43.7%, P = 0.749) nor was a difference observed for the other clinical parameters (age, gender, pain, weight loss, tumor markers level, and clinical stage). Early relapse was detected in 130 patients; local recurrence (n = 48, 36.9%) and hepatic recurrence (n = 51, 39.2%) were the most common type of relapse; other types of relapse were observed in 23.3% patients (n = 31, 23.8%). The pathological results showed that a complete R0 resection was achieved in 79% (n = 140) and 81% (n = 102) of the patients from the two medical centers, respectively. Adjuvant chemotherapy was implemented in 60·4% (n = 107) and 65·9% (n = 83) of the patients after surgery.

Intra- and Interobserver Agreement

The intraobserver reproducibility showed ICC values of 0·841 to 0·928, and the interobserver ICCs were 0·829 to 0·863. The results showed favorable intra- and interobserver reproducibility of the feature extraction.

Development of the Radiomic Signature

A total of 1312 radiomic features were extracted from each patient. Mann–Whitney tests and analysis of variance (ANOVA) tests allowed the selection of 427 features, among which 57 were identified by Spearman correlation analysis. Combined features(T_1-w+T_2-w+CET_1-w) showed higher performance than other individual sequences (Supplemental Fig. 4 and Supplemental Table 2). Finally, 10 radiomic features (two from T_1-w imaging, three from T_2-w imaging, one feature from CET_1-w arterial phase imaging and four features from CET_1-w portal vein phase imaging) were selected after LASSO regression and were used to construct the radiomic signature (Fig. 3). The details of the features and the calculation formula for the radiomic signature are shown in Supplemental Table 1 and Supplemental Fig. 1.

Evaluation Performance of the Radiomic Signature

The evaluation performance of the developed radiomic signature was assessed in the three cohorts using ROC curves (Fig. 4). In general, the value of the rad-score was significantly higher in patients who developed ER (Fig. 5 and Supplemental Fig. 2). The AUC values were 0.802 (training cohort), 0.807 (internal validation cohort), and 0.781 (external validation cohort). The boxplots of the radiomic signature distribution are shown in Supplemental Fig. 2. The details of the evaluation performance of the radiomic signature are shown in Table 3.

Development of the Radiomic Nomogram

In the univariate analysis, the carbohydrate antigen (CA) 19-9 level, clinical stage, the radiomic signature, and the total bilirubin (TB) level showed significant differences between the ER and non-ER groups in the training cohort. In multivariate logistic analysis, the radiomic signature (odds ratio [OR]: 2.535, 95% confidence interval [CI]: 1.576–4.079, $P < 0.001$), CA19-9 level (OR: 3.772, 95%

TABLE 2. Preoperative Clinical Characteristics of Patients With or Without ER

	Training cohort (*n* = 123)			Internal validation cohort (*n* = 54)			External validation cohort (*n* = 126)		
Parameters	**Non-ER (*n* = 72)**	**ER (*n* = 51)**	***P*-value**	**Non-ER (*n* = 30)**	**ER (*n* = 24)**	**P-value**	**Non-ER (*n* = 71)**	**ER (*n* = 55)**	***P*-value**
Age, years			0.835			0.924			0.808
≥ 60	41	30		18	15		42	29	
< 60	31	21		12	9		29	26	
Gender			0.580			0.799			0.102
Male	50	33		19	16		50	31	
Female	22	18		11	8		21	24	
Pain			0.575			0.454			0.909
Yes	43	33		17	16		38	30	
No	29	18		13	8		33	25	
Weight loss			0.175			0.246			0.487
Yes	32	29		14	15		33	29	
No	40	22		16	9		38	26	
Location			0.171			0.505			0.289
Proximal	56	34		20	18		55	38	
Distal	16	17		10	6		16	17	
CA199, kU/L			<0.001*			0.035*			0.001*
Normal	36	8		16	6		32	10	
Elevated	36	43		14	18		39	45	
CEA, ng/mL			0.731			0.134			0.257
Normal	59	43		28	18		61	43	
Elevated	13	8		2	6		10	12	

TABLE 2. Continued

Parameters	Training cohort (*n* = 123)			Internal validation cohort (*n* = 54)			External validation cohort (*n* = 126)		
	Non-ER (*n* = 72)	ER (*n* = 51)	*P*-value	Non-ER (*n* = 30)	ER (*n* = 24)	P-value	Non-ER (*n* = 71)	ER (*n* = 55)	*P*-value
TB, μmol/L			0.043*			0.429			0.503
Normal	43	21		17	11		41	35	
Elevated	29	30		13	13		30	20	
Albumin, g/L			0.374			0.255			0.731
Normal	52	33		21	20		47	38	
Decreased	20	18		9	4		24	17	
Stage			<0.001*			0.104			0.002*
I	39	10		15	6		31	8	
II	30	31		13	13		32	35	
III	3	10		2	5		8	12	
IV	0	0		0	0		0	0	
Radiomic signature	−1.44±0.147	0.179±0.221	<0.001*	−1.39±0.327	0.743±0.358	<0.001*	−1.13±0.155	−0.471±0.243	<0.001*

TB: total bilirubin; CEA: carcinoembryonic antigen.
*$P < 0.05$.

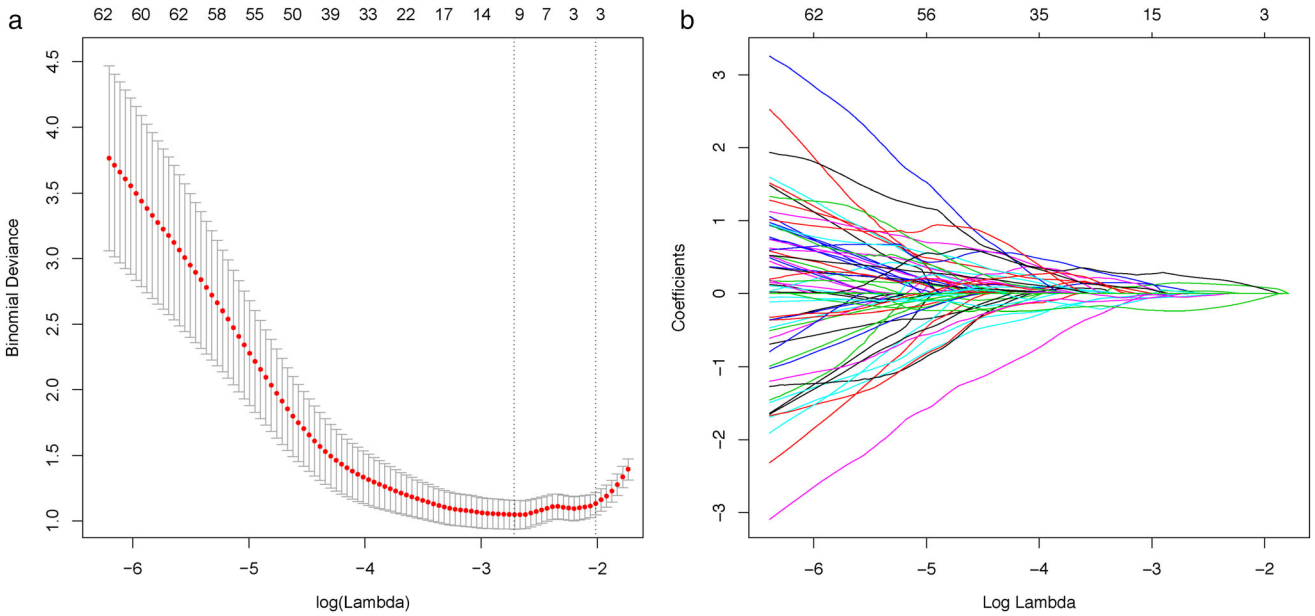

FIGURE 3: LASSO logistic regression for texture feature selection. (a) In the LASSO model, the penalization parameter λ selection used 10-fold cross-validation as the minimum criteria. The log (λ) (x-axis) was plotted against the partial likelihood deviance (y-axis). The minimum criteria and the 1-SE criteria were used to draw the dotted vertical lines at the optimal values (b). For 57 texture features, the LASSO coefficient profiles are shown. Ten-fold cross-validation in the log (λ) sequence was used to draw the vertical line at the value selected; also indicate are 10 features with nonzero coefficients.

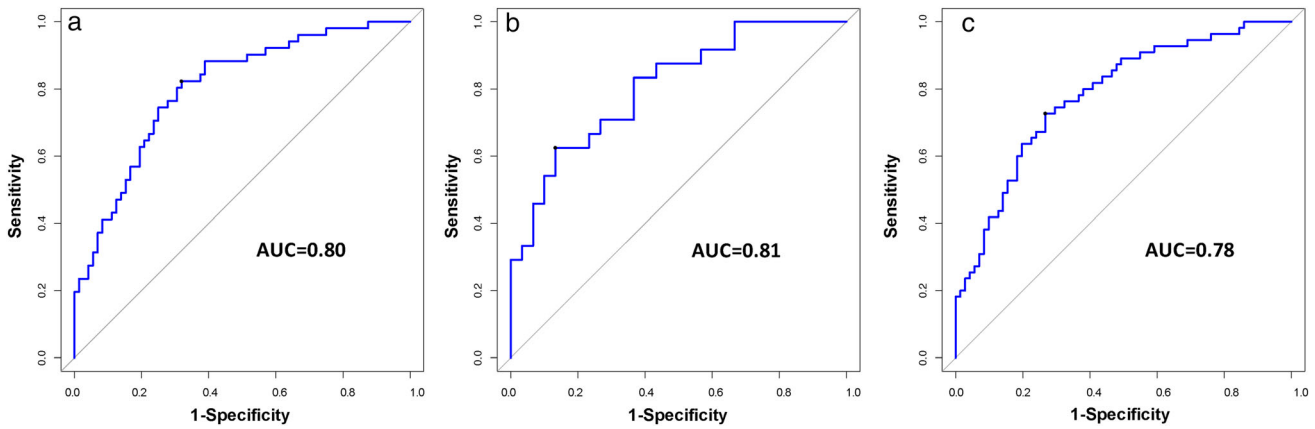

FIGURE 4: ROC curve of the ER risk evaluation performance of the radiomic signature in the training cohort (a) (AUC = 0.802) the internal validation cohort (b) (AUC = 0.807), and the external validation cohort (c) (AUC = 0·781).

CI: 1.224–11.623, P = 0.021), and clinical stage (OR: 3.748, 95% CI: 1.609–8.728, P = 0.002) were identified as independent parameters of ER. A radiomic nomogram was then developed incorporating the CA19-9 level and clinical stage. Each factor was assigned a weighted number of points. The total number of points for each patient was calculated using the nomogram, and was associated with an estimated probability of ER (Fig. 6).

Evaluation Performance of the Radiomic Nomogram

An ROC curve was used to assess the discriminative ability of the developed nomogram. The AUC values were 0.871 (training cohort), 0.876 (internal validation cohort), and 0.846 (external validation cohort) (Fig. 8 and Supplemental Fig. 3).

The radiomic nomogram showed promising evaluation performance in the three cohorts. The calibration curve indicated adequate consistency between estimated risks using the nomogram and the actual observed outcome in the three cohorts (Fig. 7). Details of the performance of radiomics nomogram are shown in Table 4.

Finally, we used a DCA curve to assess whether this nomogram would help with clinical treatment strategies (Fig. 9). In three cohorts, when the threshold probability varied from 0 to 1, according to the DCA, the radiomic nomogram achieved

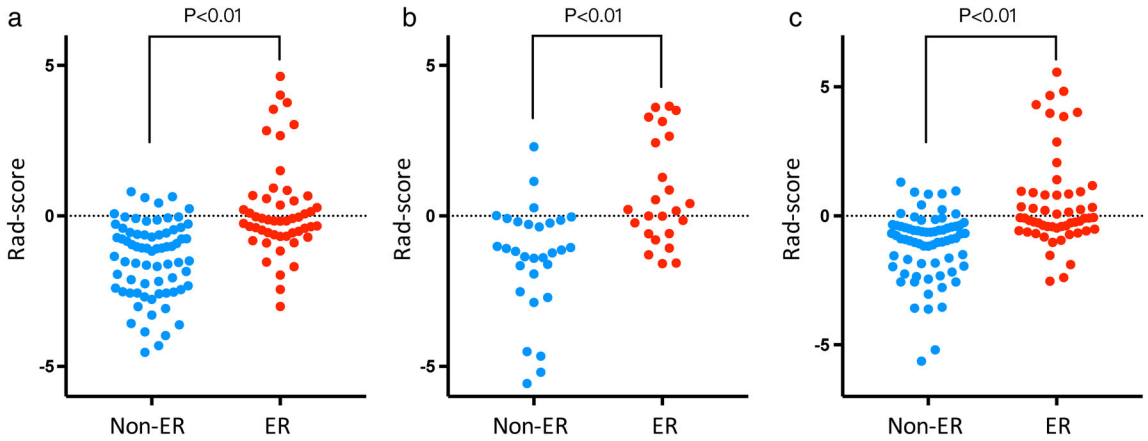

FIGURE 5: Dot diagram showing that the value of the rad-score was significantly higher in patients who developed ER in in the training cohort (a), the internal validation cohort (b), and the external validation cohort (c).

TABLE 3. Univariate and Multivariate Logistic Regression Analysis of the Radiomic Signature and Preoperative Clinical Parameters

	Univariate analysis			Multivariate analysis		
Parameters	**OR**	**95% CI**	***P***	**OR**	**95% CI**	***P***
Radiomics signature	2.840	1.796–4.489	< 0.001*	2.535	1.576–4.079	< 0.001*
Age ≥ 60 years	0.926	0.447–1.915	0.835			
Pain	1.141	0.716–1.819	0.575			
Weight loss	1.288	0.884–1.877	0.175			
Gender	1.073	0.832–1.384	0.580			
Location	1.750	0.783-3.913	0.171			
CA19-9 > 37kU/L	5.375	2.219–13.021	< 0.001*	3.772	1.224–11.623	0.021*
CEA > 3.4ng/mL	1.151	0.515–2.573	0.731			
TB > 17.1 μmol/L	2.118	1.021–4.395	0.043*	1.867	0.688–5.065	0.220
Albumin < 35 g/L	1.418	0.655–3.069	0.374			
TNM stage	3.764	1.950–7.266	< 0.001*	3.748	1.609–8.728	0.002*

CEA, carcinoembryonic antigen; TB, total bilirubin; CI, confidence internal.
Significant parameters with $P < 0.05$ in the univariate analysis were included in the multivariate logistic regression analysis.

the most net benefit compared with a "treat all" strategy, a "treat none" strategy, and the radiomic signature.

Discussion

Pancreatic cancer has a poor prognosis, even after surgery. The recurrence rate and survival for patients in identical stages vary greatly.[17,18] This evidence indicates that PC is a heterogeneous disease and upfront surgery is not suitable for the subgroup of patients with increased risk of ER, even in the early stage.[19,20] Neoadjuvant chemotherapy (NAC) might be an optimal choice for these patients and could help to eliminate the circulating tumor cells and distant micrometastatic lesions, leading to a reduced ER rate after surgery.[21] Accumulating evidence demonstrates that patients with BRPC and LAPC could obtain remarkable survival benefit from NAC.[22,23] Thus, some physicians have started to use NAC in resectable cases.[24] In guidelines proposed by the National Comprehensive Cancer Network (NCCN), NAC is recommended for high-risk resectable PC.[25] However, whether patients with resectable pancreatic cancer (RPC) should receive NAC remains controversial. One of the main challenges is that we lack methods to identify patients who could benefit from upfront surgery. Except for CA19-9, a severely limited biomarker, no viable prognostic or predictive biomarkers for PC are currently available.[26]

TABLE 4. Predictive Performance of the Radiomic Signature and Radiomic Nomogram

Model	Radiomic signature			Clinical characteristics			Radiomic nomogram		
	Specificity	Sensitivity	AUC (95% CI)	Specificity	Sensitivity	AUC (95% CI)	Specificity	Sensitivity	AUC (95% CI)
Training cohort	0.681	0.824	0.802 (0.721–0.868)	73.61	70.59	0.757(0.672–0.830)	0.611	0.961	0.871 (0.799–0.925)
Internal validation cohort	0.867	0.625	0.807 (0.677–0.902)	76.67	62.50	0.739(0.601–0.849)	0.933	0.667	0.876 (0.758–0.950)
Independent validation	0.727	0.732	0.781 (0.699–0.850)	70.91	66.20	0.718(0.631–0.795)	0.803	0.746	0.846 (0.771–0.904)

AUC, area under the receiver operating characteristic (ROC) curve; CI, confidence interval.

In the present study we sought to develop a preoperative radiomic nomogram to help identify patients with increased risk of ER. The texture features in our radiomic signature included both high- and low-order radiomic features, which were consistent with previous studies. Histogram parameters (a low-order radiomic feature), which are related to the properties of individual pixels, describe the distribution of voxel intensities within an image via commonly used and basic metrics.[27] Histogram feature such as intensity, kurtosis, and skewness, based on enhanced MRI images, reflect the enhancement ratio of a tumor. Previous studies demonstrated that the hypoattenuation value parameter is likely to reflect the degree of tumor necrosis within the tumor tissue and an isoattenuating enhancement pattern might represent a relatively well-differentiated and less aggressive tumor.[28,29] High-order radiomic features, such as GLCM features, measure the spatial relationship between local nearby pixels.[30] We assumed that high-order features better reflect the tumor biology and heterogeneity. The prognostic value of the high-order radiomic texture of MRI has also been proven in various malignancies, including breast cancer, hepatocellular carcinoma, and nasopharyngeal carcinoma.[31–33] A study of preoperative MRI texture analysis conducted by Choi et al showed that tumor size and entropy with medium texture were significantly associated with overall survival in patients with pancreatic ductal adenocarcinoma (PDAC).[34] However, it remains a challenge to associate a single radiomic feature with complex tumor biological processes. Therefore, to perform outcome estimation in the –omics setting, it is more common to construct multifactor panels. Our results showed that the developed radiomic signature achieved satisfactory risk evaluation results for ER in the primary and external cohorts.

We then constructed a radiomic nomogram that incorporated clinical factors (the CA19-9 level and clinical stage) and the radiomic signature, which showed favorable performance and improved risk evaluation accuracy in both the internal and external independent cohorts.

CA-199 was identified as an independent prognostic predictor in this study, which was consistent with previous studies.[35–37] The level of CA19-9 correlates closely with disease burden in patients, and a higher CA19-9 value indicates an increased risk of tumor metastasis. However, CA19-9 as a marker has limitations. For example, CA19-9 is often elevated in patients with jaundice, which could result in overestimation of the disease burden.[26] Moreover, CA19-9 levels correlate poorly with tumor differentiation, which is highly associated with prognosis in PC.[38] In our study, CA19-9 alone archived an AUC of 0.672 for discrimination of ER in the training cohort. Therefore, CA19-9 alone is not enough for accurate risk assessment of ER.

The clinical stage system stratifies PDAC according to three major parameters on images: primary tumor, regional lymph nodes, and distant metastases.[5] This criterion is

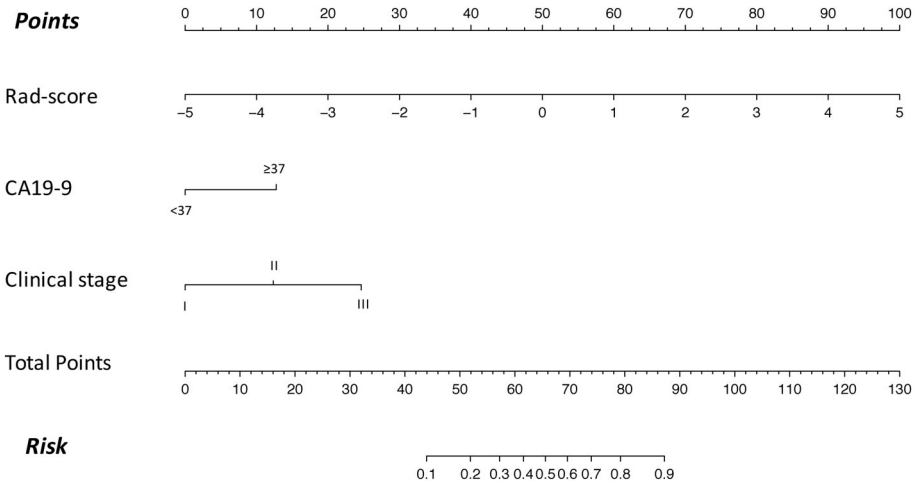

FIGURE 6: The radiomic nomogram incorporating the radiomic signature, the CA19-9 level, and the clinical stage.

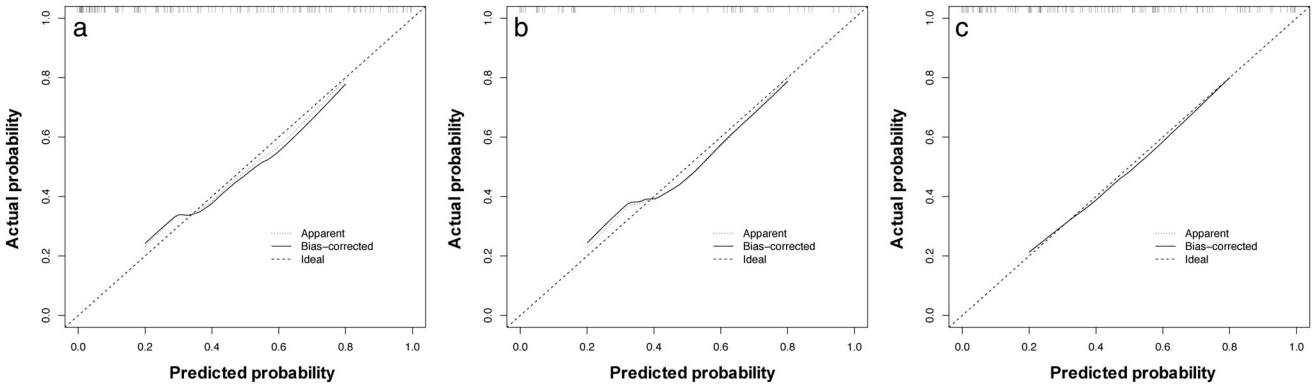

FIGURE 7: Calibration curves for the nomogram in the training cohort (a), the internal validation cohort (b), and the external validation cohort (c). The 45° black line represents the reference line showing the "ideal" prediction. The dotted line indicates the performance of the radiomic nomogram in ER prediction, and the solid line indicates the correction of bias in the radiomic nomogram.

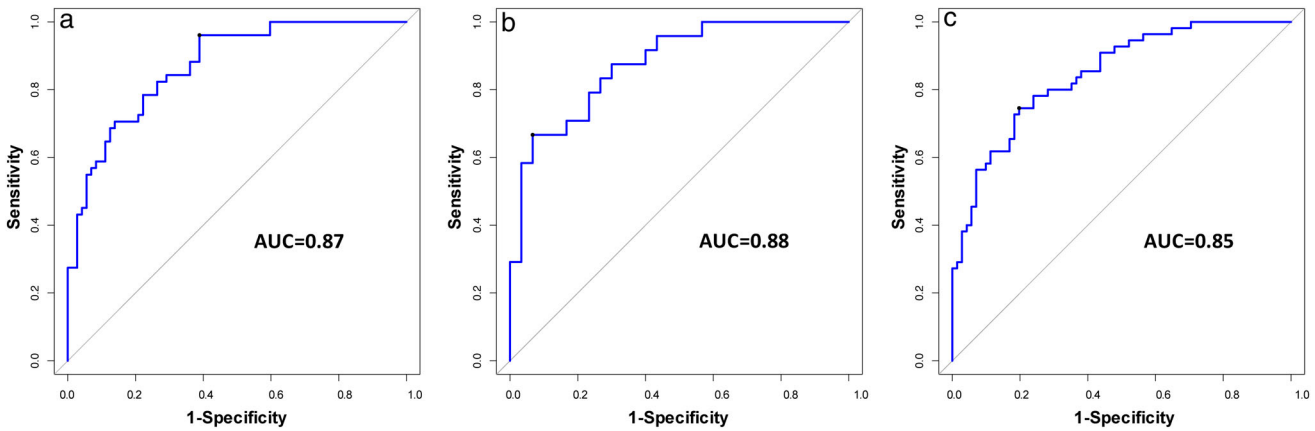

FIGURE 8: ROC curve of the ER risk evaluation performance of the radiomic nomogram in the training cohort (a) (AUC = 0·871) the internal validation cohort (b) (AUC = 0·876), and the external validation cohort (c) (AUC = 0·846).

fundamental to establish a prognosis in different malignancies. In the present study, we observed that patients in the later stage are more likely to have ER after surgery. However, the clinical stage system mainly focuses on anatomical radiological features, which might oversimplify the complexity of a tumor's biological behavior. Therefore, clinical stage alone is not enough for accurate risk evaluation of ER.

According to previous studies of PC, severe pain and obvious weight loss were also associated with poor prognosis.[39,40] However, our data failed to confirm these results.

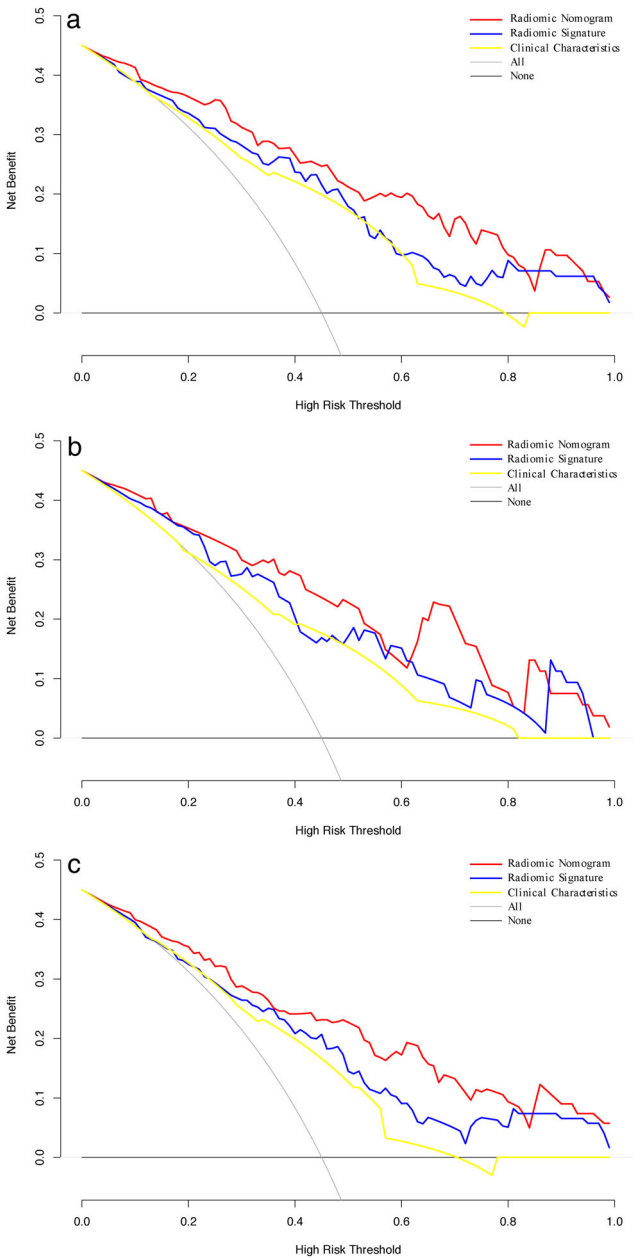

FIGURE 9: DCA curve of clinical use assessment of the radiomic signature and the radiomic nomogram in the training cohort (a), internal validation cohort (b), and external validation cohort (c). The net benefit is shown on the y-axis and the threshold probability is shown on the x-axis. Use of the radiomic nomogram (red line) achieves the highest net benefit compared with the radiomic signature (blue line), clinical characteristics (yellow line), treat-all strategy (gray line), and the treat-none strategy (horizontal black line).

Pain can be related to infiltration of a tumor into surrounding nerves, vessels, or viscera. Different types of invasion can have varying impacts on prognosis. However, parameters such as pain might be subjective because of varying levels of sensitivity among patients to abdominal pain caused by the tumor. Weight loss indicates the malnutrition status of patients. In the present study, we observed a lower rate of weight loss compared with that in previous reports.[40] This could be related to the diverse ethnic population included. The tumors were identified by physical examination in many patients included in our study and were at an early stage without symptoms, which could also account for these results.

Finally, DCA showed that the radiomic nomogram outperformed the radiomic signature across a wide range of threshold probabilities, which revealed that the clinical parameters added incremental value to ER risk evaluation in both the primary and external cohorts.

The developed risk evaluation model has obvious advantages. Compared with gene expression tests based on invasive biopsies, the noninvasive characteristic of radiomic analysis lends itself to a wide range of applications for patients. In addition, biopsies have obvious limitations caused by sampling bias that could result from intratumoral heterogeneity, while radiomics represents a comprehensive assessment of the whole tumor. Moreover, the preoperative data used in the developed risk evaluation model are easily accessible, with little additional cost and show favorable results. These advantages and results are encouraging and promising.

Limitations

Our study has several limitations. First, selection bias might exist because of the retrospective design of our study. Second, this was a relatively small sample size. However, our cohort is still one of the largest with respect to radiomics and resectable PC. Third, we abandoned the diffusion-weighted MR image with different b values over a long time period because of poor consistency between the two hospitals. The T_1-w, T_2-w, portal venous phase, and arterial phase were chosen to ensure that the cohorts were large enough to develop a stable model to evaluate ER risks.

Conclusion

We developed a novel model incorporating a radiomic signature and clinical parameters to evaluate the ER risks of patients with resectable PC preoperatively. The accurate identification of this subgroup of early-stage patients who would receive little benefit from upfront surgery might potentially help decision-making for treatment strategies and clinical trials. Although the results are encouraging and promising, further validation of this evaluation model in a large and diverse population is still required.

Acknowledgment

We thank Jianfeng Wang for assistance in the study.

Contract grant sponsor: National High Technology Research and Development Program of China; Contract grant number: SS2015AA020405; Contract grant sponsor: National Natural Science Foundation of China; Contract grant numbers: 81672337, 81871925, 81702332; Contract grant sponsor: Key Program of the National Natural Science

Foundation of China; Contract grant number: 81530079; Contract grant sponsor: Key Research and Development Project of Zhejiang Province; Contract grant number: 2015C03044; Contract grant sponsor: Zhejiang Provincial Program for the Cultivation of High-level Innovative Health talents.

References

1. Groot VP, Gemenetzis G, Blair AB, et al. Defining and predicting early recurrence in 957 patients with resected pancreatic ductal adenocarcinoma. Ann Surg 2019;269:1154–1162.
2. Yamamoto Y, Ikoma H, Morimura R, et al. Optimal duration of the early and late recurrence of pancreatic cancer after pancreatectomy based on the difference in the prognosis. Pancreatology 2014;14:524–529.
3. Nishio K, Kimura K, Amano R, et al. Preoperative predictors for early recurrence of resectable pancreatic cancer. World J Surg Oncol 2017; 15:16.
4. Allen PJ, Kuk D, Castillo CF, et al. Multi-institutional validation study of the American Joint Commission on Cancer (8th edition) changes for T and N staging in patients with pancreatic adenocarcinoma. Ann Surg 2017;265:185–191.
5. Kamarajah SK, Burns WR, Frankel TL, Cho CS, Nathan H. Validation of the American Joint Commission on Cancer (AJCC) 8th edition staging system for patients with pancreatic adenocarcinoma: A surveillance, epidemiology and end results (SEER) analysis. Ann Surg Oncol 2017; 24:2023–2030.
6. Lambin P, Rios-Velazquez E, Leijenaar R, et al. Radiomics: Extracting more information from medical images using advanced feature analysis. Eur J Cancer 2012;48:441–446.
7. Wei J, Yang G, Hao X, et al. A multi-sequence and habitat-based MRI radiomics signature for preoperative prediction of MGMT promoter methylation in astrocytomas with prognostic implication. Eur Radiol 2019;29:877–888.
8. Jiang Y, Chen C, Xie J, et al. Radiomics signature of computed tomography imaging for prediction of survival and chemotherapeutic benefits in gastric cancer. EBioMedicine 2018;36:171–182.
9. Huang YQ, Liang CH, He L, et al. Development and validation of a radiomics nomogram for preoperative prediction of lymph node metastasis in colorectal cancer. J Clin Oncol 2016;34:2157–2164.
10. Liu Z, Zhang XY, Shi YJ, et al. Radiomics analysis for evaluation of pathological complete response to neoadjuvant chemoradiotherapy in locally advanced rectal cancer. Clin Cancer Res 2017;23:7253–7262.
11. Yin P, Mao N, Liu X, et al. Can clinical radiomics nomogram based on 3D multiparametric MRI features and clinical characteristics estimate early recurrence of pelvic chondrosarcoma? J Magn Reson Imaging 2019 doi: https://doi.org/10.1002/jmri.26834 [Epub ahead of print].
12. Zhang Z, Jiang H, Chen J, et al. Hepatocellular carcinoma: Radiomics nomogram on gadoxetic acid-enhanced MR imaging for early postoperative recurrence prediction. Cancer Imaging 2019;19:22.
13. Liang W, Xu L, Yang P, et al. Novel nomogram for preoperative prediction of early recurrence in intrahepatic cholangiocarcinoma. Front Oncol 2018;8:360.
14. Kaissis G, Ziegelmayer S, Lohofer F, et al. A machine learning model for the prediction of survival and tumor subtype in pancreatic ductal adenocarcinoma from preoperative diffusion-weighted imaging. Eur Radiol Exp 2019;3:41.
15. Kaissis G, Ziegelmayer S, Lohofer F, et al. A machine learning algorithm predicts molecular subtypes in pancreatic ductal adenocarcinoma with differential response to gemcitabine-based versus FOLFIRINOX chemotherapy. PLoS One 2019;14:e0218642.
16. Yushkevich PA, Piven J, Hazlett HC, et al. User-guided 3D active contour segmentation of anatomical structures: Significantly improved efficiency and reliability. Neuroimage 2006;31:1116–1128.
17. Stark AP, Sacks GD, Rochefort MM, et al. Long-term survival in patients with pancreatic ductal adenocarcinoma. Surgery 2016;159:1520–1527.
18. Rochefort MM, Ankeny JS, Kadera BE, et al. Impact of tumor grade on pancreatic cancer prognosis: Validation of a novel TNMG staging system. Ann Surg Oncol 2013;20:4322–4329.
19. Cros J, Raffenne J, Couvelard A, Pote N. Tumor heterogeneity in pancreatic adenocarcinoma. Pathobiology 2018;85:64–71.
20. Kurahara H, Maemura K, Mataki Y, et al. A therapeutic strategy for resectable pancreatic cancer based on risk factors of early recurrence. Pancreas 2018;47:753–758.
21. Gillen S, Schuster T, Meyer Zum Büschenfelde C, Friess H, Kleeff J. Preoperative/neoadjuvant therapy in pancreatic cancer: A systematic review and meta-analysis of response and resection percentages. PLoS Med 2010;7:e1000267.
22. Hackert T, Sachsenmaier M, Hinz U, et al. Locally advanced pancreatic cancer: Neoadjuvant therapy with FOLFIRINOX results in resectability in 60% of the patients. Ann Surg 2016;264:457–463.
23. Blazer M, Wu C, Goldberg RM, et al. Neoadjuvant modified (m) FOLFIRINOX for locally advanced unresectable (LAPC) and borderline resectable (BRPC) adenocarcinoma of the pancreas. Ann Surg Oncol 2015;22:1153–1159.
24. Evans DB, Multidisciplinary Pancreatic Cancer Study G. Resectable pancreatic cancer: The role for neoadjuvant/preoperative therapy. HPB 2006;8:365–368.
25. Tempero MA, Malafa MP, Chiorean EG, et al. Pancreatic adenocarcinoma, version 1.2019. J Natl Compr Canc Netw 2019;17:202–210.
26. Goh SK, Gold G, Christophi C, Muralidharan V. Serum carbohydrate antigen 19-9 in pancreatic adenocarcinoma: A mini review for surgeons. ANZ J Surg 2017;87:987–992.
27. Vidic I, Egnell L, Jerome NP, et al. Support vector machine for breast cancer classification using diffusion-weighted MRI histogram features: Preliminary study. J Magn Reson Imaging 2018;47:1205–1216.
28. Takumi K, Fukukura Y, Higashi M, et al. Pancreatic neuroendocrine tumors: Correlation between the contrast-enhanced computed tomography features and the pathological tumor grade. Eur J Radiol 2015;84: 1436–1443.
29. Sandrasegaran K, Lin Y, Asare-Sawiri M, Taiyini T, Tann M. CT texture analysis of pancreatic cancer. Eur Radiol 2019;29:1067–1073.
30. Fathi Kazerooni A, Nabil M, Haghighat Khah H, et al. ADC-derived spatial features can accurately classify adnexal lesions. J Magn Reson Imaging 2018;47:1061–1071.
31. Kim JH, Ko ES, Lim Y, et al. Breast cancer heterogeneity: MR imaging texture analysis and survival outcomes. Radiology 2017;282:665–675.
32. Zhang J, Liu X, Zhang H, et al. Texture analysis based on preoperative magnetic resonance imaging (MRI) and conventional MRI features for predicting the early recurrence of single hepatocellular carcinoma after hepatectomy. Acad Radiol 2019;26:1164–1173.
33. Hocquelet A, Auriac T, Perier C, et al. Pre-treatment magnetic resonance-based texture features as potential imaging biomarkers for predicting event free survival in anal cancer treated by chemoradiotherapy. Eur Radiol 2018;28:2801–2811.
34. Choi MH, Lee YJ, Yoon SB, Choi JI, Jung SE, Rha SE. MRI of pancreatic ductal adenocarcinoma: Texture analysis of T2-weighted images for predicting long-term outcome. Abdom Radiol 2019;44:122–130.
35. Duffy MJ, Sturgeon C, Lamerz R, et al. Tumor markers in pancreatic cancer: A European Group on Tumor Markers (EGTM) status report. Ann Oncol 2010;21:441–447.
36. Waraya M, Yamashita K, Katagiri H, et al. Preoperative serum CA19-9 and dissected peripancreatic tissue margin as determiners of long-term survival in pancreatic cancer. Ann Surg Oncol 2009;16:1231–1240.
37. Berger AC, Meszoely IM, Ross EA, Watson JC, Hoffman JP. Undetectable preoperative levels of serum CA 19-9 correlate with improved survival for patients with resectable pancreatic adenocarcinoma. Ann Surg Oncol 2004;11:644–649.

38. Chan A, Prassas I, Dimitromanolakis A, et al. Validation of biomarkers that complement CA19.9 in detecting early pancreatic cancer. Clin Cancer Res 2014;20:5787–5795.

39. Carr RA, Roch AM, Zhong X, et al. Prospective evaluation of associations between cancer-related pain and perineural invasion in patients with resectable pancreatic adenocarcinoma. J Gastrointest Surg 2017; 21:1658–1665.

40. Olson SH, Xu Y, Herzog K, et al. Weight loss, diabetes, fatigue, and depression preceding pancreatic cancer. Pancreas 2016;45: 986–991.